Doublecortin facilitates the elongation of the somatic Golgi apparatus into proximal dendrites

Peijun Li[a], Luyao Li[a], Binyuan Yu[a], Xinye Wang[a], Qi Wang[a], Jingjing Lin[a], Yihui Zheng[a], Jinjin Zhu[a], Minzhi He[a], Zhaonan Xia[a], Mengjing Tu[a], Judy S. Liu[b,†], Zhenlang Lin[a,*], and Xiaoqin Fu[a,†,*]

[a]The Second Affiliated Hospital and Yuying Children's Hospital, Wenzhou Medical University, Wenzhou, Zhejiang 325000, China; [b]Department of Neurology, Department of Molecular Biology, Cell Biology, and Biochemistry, Brown University, Providence, RI 02903

ABSTRACT **Mutations in the doublecortin (*DCX*) gene, which encodes a microtubule (MT)-binding protein, cause human cortical malformations, including lissencephaly and subcortical band heterotopia. A deficiency in DCX and DCX-like kinase 1 (DCLK1), a functionally redundant and structurally similar cognate of DCX, decreases neurite length and increases the number of primary neurites directly arising from the soma. The underlying mechanism is not completely understood. In this study, the elongation of the somatic Golgi apparatus into proximal dendrites, which have been implicated in dendrite patterning, was significantly decreased in the absence of DCX/DCLK1. Phosphorylation of DCX at S47 or S327 was involved in this process. DCX deficiency shifted the distribution of CLASP2 proteins to the soma from the dendrites. In addition to CLASP2, dynein and its cofactor JIP3 were abnormally distributed in DCX-deficient neurons. The association between JIP3 and dynein was significantly increased in the absence of DCX. Down-regulation of CLASP2 or JIP3 expression with specific shRNAs rescued the Golgi phenotype observed in DCX-deficient neurons. We conclude that DCX regulates the elongation of the Golgi apparatus into proximal dendrites through MT-associated proteins and motors.**

Monitoring Editor
Paul Forscher
Yale University

Received: Sep 17, 2019
Revised: Dec 23, 2020
Accepted: Dec 30, 2020

INTRODUCTION

During neuronal development, migrating cells undergo a series of shape changes before they reach their final positions and morphology. As a major cytoskeletal component, microtubules (MTs) and their associated proteins play crucial roles in this process. Therefore, many causative genes for neuronal migration disorders are unsurprisingly related to MTs. Doublecortin (*DCX*), a gene encoding an MT-binding protein, is one of the causative genes for lissencephaly, which is characterized by a "smooth cortex" resulting from abnormal neuronal migration (des Portes *et al.*, 1998; Gleeson *et al.*, 1998). Other causative genes for lissencephaly include *TUBA1A* (Keays *et al.*, 2007), cytoplasmic dynein heavy chain (*DHC;* Poirier *et al.*, 2013), *LIS1* (Reiner *et al.*, 1993), *ARX*, and *RELN*. Of these genes, *DCX, KINESIN-3, TUBA1A, LIS1*, and *DHC* all encode proteins that directly interact with the MT cytoskeleton, including MAPs and motors.

The functions of DCX are closely related to MTs, including stabilizing the MT structure and exerting cooperative binding effects on MTs (Horesh *et al.*, 1999; Akhmanova and Severin, 2004; Moores *et al.*, 2004; Moores *et al.*, 2006). DCX also regulates the MT-related molecular motor kinesin-3 and associated intracellular trafficking (Deuel *et al.*, 2006; Liu *et al.*, 2012; Lipka *et al.*, 2016). In addition, DCX and DCDC5, another DCX family protein, interact with dynein, which is another important MT-related molecular motor that is exclusively required for MT minus-end directed transport (Tanaka *et al.*, 2004a; Kaplan and Reiner, 2011).

DCX/DCLK1 deficiency decreases the neurite length and increases the number of primary neurites directly arising from the soma (Liu *et al.*, 2012). The Golgi complex plays important roles in dendrite patterning (Horton and Ehlers, 2003; Horton *et al.*, 2005; Ye *et al.*, 2007; Ori-McKenney *et al.*, 2012; Zhou *et al.*, 2014). In

This article was published online ahead of print in MBoC in Press (http://www.molbiolcell.org/cgi/doi/10.1091/mbc.E19-09-0530) on January 6, 2021.

†These authors contributed equally to the work.

The authors have no conflicts of interest related to the contents of this article to declare.

*Address correspondence to: Xiaoqin Fu (fuxq@wzhealth.com); Zhenlang Lin (linzhenlang@hotmail.com).

Abbreviations used: DCX, doublecortin; DHC, dynein heavy chain; KO, knockout; MS, mass spectrometry; MT, microtubule; WT, wild type.

nonneuronal cells, the Golgi apparatus is located near the nucleus as a compact structure. In many neurons, however, the somatic Golgi apparatus extends into proximal dendrites, and the Golgi structure is observed in distal dendrites. The Golgi complex directly nucleates MTs in neurons, promotes the growth of dendrite branches, and maintains their stability (Ori-McKenney *et al.*, 2012). In the present study, the extension of the Golgi complex into proximal dendrites was significantly decreased in DCX-deficient neurons. In the absence of DCX, abnormalities were also observed in CLASP2, dynein, and JIP3. Down-regulation of CLASP2 or JIP3 rescued the Golgi phenotype in DCX-deficient neurons. We conclude that DCX regulates Golgi extension in proximal dendrites through multiple mechanisms.

RESULTS

The extension of the somatic Golgi apparatus into proximal dendrites was significantly decreased in DCX-deficient neurons

A DCX/DCLK1 deficiency decreases the neurite length and increases the number of primary neurites directly arising from the soma (Liu *et al.*, 2012). We examined the distribution of the Golgi complex by staining neurons from wild-type (WT) or *Dcx-/y;Dclk1–/–* mice for GM130, an endogenous Golgi matrix protein, to determine whether the Golgi plays a role in the neuronal morphology defects observed in DCX/DCLK1-deficient neurons. In addition to its location in the cell body, the somatic Golgi apparatus usually extends into proximal dendrites in neurons. The somatic Golgi complex was mainly restricted to the soma in DCX/DCLK1-deficient neurons compared with WT neurons (Figure 1A). The distance from the Golgi apparatus to the nucleus was measured from the distal edge of the somatic Golgi apparatus to the closest edge of the nucleus to quantify the Golgi phenotype (Figure 1B). The distance from the somatic Golgi complex to the nucleus was significantly decreased in neurons lacking DCX/DCLK1 (Figure 1C). In addition, the MT organizing center or centrosome retained its normal association with the Golgi in these neurons, but it was retained in the cell body instead of being translocated into the leading dendrite, as observed in WT neurons (Figure 1, D and E). Electron microscopy of the cortex revealed a similar Golgi structure in *Dcx-/y;Dclk1–/–* mice and WT mice (Figure 1F), revealing a relatively intact morphology of the organelle, including the stacks, despite the abnormal position of the Golgi. Moreover, the decrease in DCX levels mediated by the DCX shRNA in WT neurons significantly decreased the dendritic distribution of the somatic Golgi complex compared with controls (Figure 2, A, B, and E). Immunostaining for DCX (bottom picture in Figure 2B) failed to detect DCX in a neuron transfected with the plasmid expressing the DCX shRNA and GFP, while DCX was detected in neurons transfected with the plasmid expressing the control shRNA (bottom picture of Figure 2A). Quantification of DCX levels from immunostaining images indicated that DCX levels were decreased by (87 ± 8)% in neurons expressing the DCX shRNA by 3 d after transfection (based on 50 transfected neurons) compared with controls.

DCX reintroduction rescued the Golgi phenotype, and more Golgi apparatuses were observed in proximal dendrites, indicating that the effect on the Golgi complex was not an off-target effect (Figure 2, C and E).

Inhibition of the phosphorylation of DCX at S47 or S327 disrupted the rescue of the Golgi phenotype

Several signaling pathways induce DCX phosphorylation at different serine/threonine residues (Figure 2D). CDK5 phosphorylates DCX on S28, S334, or S297 (Graham *et al.*, 2004; Tanaka *et al.*, 2004b); MAPK2 and PKA mainly phosphorylate DCX on S47 (Schaar *et al.*, 2004); JNK phosphorylates DCX on T321, T331, and S334 (Gdalyahu *et al.*, 2004); and JIP3/GSK3-β phosphorylate DCX on S327 (Bilimoria *et al.*, 2010). We used nonphosphorylatable DCX mutants that mimic the conformation of dephosphorylated DCX, S297A, S47A, or S327A to test which mutant may affect the rescue of the Golgi phenotype and determine the effect of DCX phosphorylation on the Golgi phenotype. S47A and S327A did not rescue the Golgi phenotype in DCX-deficient neurons, while S297A expression completely restored Golgi complex extension in proximal dendrites (Figure 2F). Furthermore, DCX S327A did not rescue and further decreased the elongation of the Golgi complex into proximal dendrites ($P = 0.035$), indicating a dominant negative effect. Therefore, phosphorylation of DCX at S47 or S327 is important for promoting Golgi complex extension in proximal dendrites. Both the MAPK2/PKA and the GSK3-β signaling pathways might be involved in the effects of DCX on the Golgi distribution in neurons. JIP3 regulates the phosphorylation of DCX at S327 through GSK3-β to control axonal branches (Bilimoria *et al.*, 2010). GSK3-β might be a critical factor influencing the Golgi distribution in neurons, and more experiments are needed in the future to confirm this hypothesis.

CLASP2 was involved in the effects of DCX on the Golgi

According to previous studies, overexpression of CLASP2 decreases the amount of the Golgi ribbon structure in dendrites and increases the number of Golgi stacks in the cell body (Beffert *et al.*, 2012). Moreover, CLASP2 is an essential Reelin effector that influences the cytoskeleton during brain development (Dillon *et al.*, 2017). Based on these findings, we assessed whether CLASP2 was involved in the effects of DCX on the Golgi distribution. We first examined the localization of CLASP2 and DCX in neurons. Immunostaining showed a very similar distribution of CLASP2 and DCX in the cell body and distal dendrites (Figure 3A). However, a direct interaction between CLASP2 and DCX was not detected using IP and Western blot analyses (Supplemental Data). Based on the immunofluorescence staining, both DCX and CLASP2 partially colocalized with GM130-stained Golgi structures (Figure 3, B and C), consistent with a previous report (Beffert *et al.*, 2012). The CLASP2 intensity in dendrites was quantified along the trajectories of neural processes starting from the soma and extending out 50 μm (shown as a broken white line adjacent to the neurite in Figure 3D). Significantly ($p < 0.01$) lower levels of CLASP2 were observed starting at 5 μm from the cell body of DCX-deficient neurons ($n = 42$) compared with the controls ($n = 47$) (Figure 3F). CLASP2 levels were also quantified in the soma and were increased in the soma of DCX-deficient neurons compared with controls (Figure 3E). DCX staining showed that the DCX shRNA successfully down-regulated DCX levels in a transfected cell (white arrow in the third row of Figure 3D) compared with a nontransfected cell (purple arrow in the third row of Figure 3D), while the DCX level in a control shRNA-transfected cell (white arrow in the first row of Figure 3D) was similar to a nontransfected cell (purple arrow in the first row of Figure 3D). Western blotting results did not reveal a change in the total levels of CLASP2 protein in DCX-deficient neurons compared with controls (data not shown). Then, we used a bi-cistronic-GFP vector expressing a CLASP2-specific shRNA whose efficacy in CLASP2 knockdown was previously validated in DCX-deficient neurons (Table 1) (Beffert *et al.*, 2012). CLASP2 silencing completely rescued the Golgi phenotype caused by the DCX deficiency, as depicted in Figure 3G. Based on the results, CLASP2 is involved in the effects of DCX on Golgi extension into dendrites.

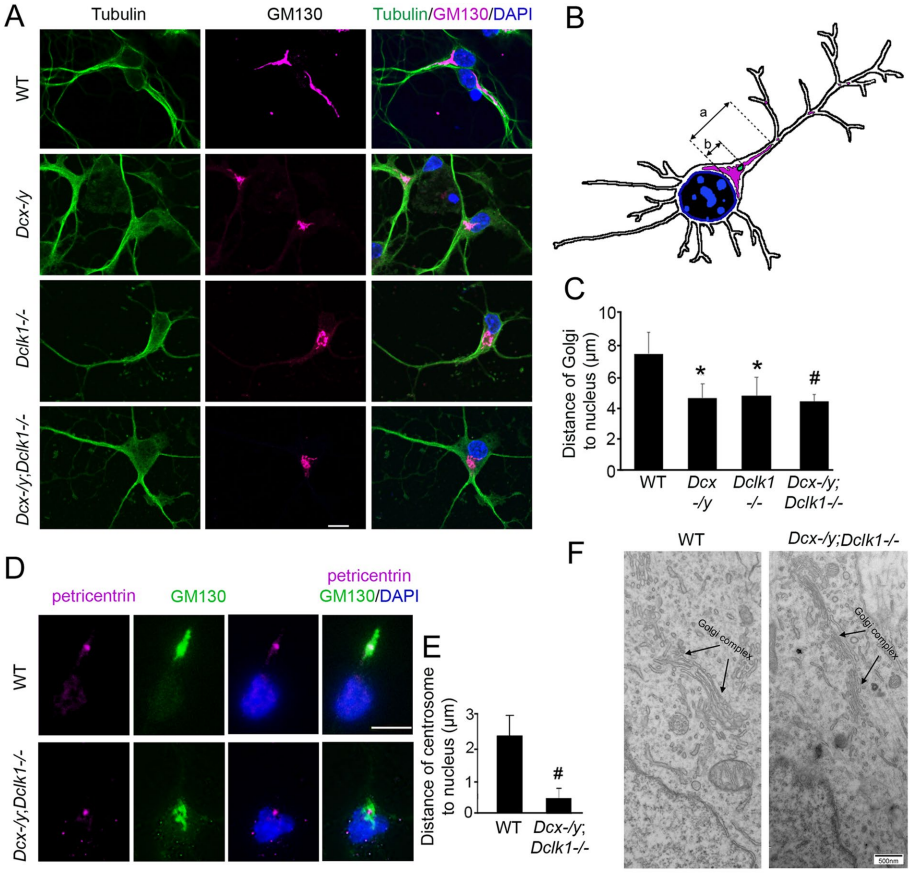

FIGURE 1: The dendritic localization of the Golgi is impaired in DCX-deficient neurons. (A) Cultured hippocampal neurons from WT or *Dcx-/y* and *Dclk1–/–* single and double mutant mice were stained for GM130 (purple), tubulin (green), and DAPI (blue) on DIV4. A WT neuron has a somatic Golgi apparatus (GM130 staining) extended into the dendrite. In the *Dcx/Dclk1* mutant neurons, most of the Golgi apparatus did not extend into the dendrite. The scale bar represents 10 μm. (B) Schematic of the measurement of the distance from the somatic Golgi apparatus or centrosome to the nucleus: the distances were measured from the distal edge of the somatic Golgi apparatus or the center of the centrosome to the closest edge of the nucleus, and indicated as "a" or "b," respectively. (C) The distances of the somatic Golgi apparatus to the nucleus were quantified and compared among WT ($n = 189$), *Dcx-/y* ($n = 213$), *Dclk1–/–* ($n = 156$), or *Dcx-/y;Dclk1–/–* ($n = 163$) neurons. (D) The centrosome remained associated with the Golgi in *Dcx/Dclk1* mutant neurons. The scale bar represents 10 μm. (E) Similar to the Golgi, the translocation of the centrosome into the primary dendrite was impaired in *Dcx/Dclk1* mutant neurons. (F) Representative electron microscopy images of the WT and *Dcx-/y;Dclk1–/–* cortex showing Golgi structure (indicated with arrows). Data were obtained from four independent experiments. *$P < 0.05$; #$P < 0.01$; P values were calculated from t tests.

MT motors and the Golgi distribution in dendrites

As shown in our previous studies, DCX specifically regulates the MT motor kinesin-3, which is also encoded by a causative gene for lissencephaly (Deuel *et al.*, 2006; Liu *et al.*, 2012). Another kinesin, MT motor kinesin-1, affects the dendritic distribution of the Golgi (Kelliher *et al.*, 2018), and kinesin-3 cotransports some cargos with kinesin-1 (Hendricks *et al.*, 2010; Guardia *et al.*, 2016; Lim *et al.*, 2017). Neuronal cultures were stained with antisera for kinesin-3 and the Golgi marker giantin, showing that kinesin-3 was widely distributed within the cell and displayed some colocalization with the Golgi (Figure 4A). We transfected cultured neurons with a kinesin-3 shRNA (Tsai *et al.*, 2010; Liu *et al.*, 2012) and stained the Golgi with the GM130 antibody. Expression of the kinesin-3 shRNA significantly decreased the distribution of the Golgi apparatus in dendrites (Figure 4, B and C). As shown in our previous studies, DCX regulates kinesin-3 and its transport of VAMP2. Further investigations are needed to determine whether kinesin-3 is directly involved in the effects of DCX on Golgi extension into dendrites. In addition to interacting with kinesin-3, DCX interacts with another MT motor, dynein, which is the major MT motor mediating retrograde transport in neuronal axons (Tanaka *et al.*, 2004a). Dynein and its cofactor NudE also regulate the distribution of Golgi outposts in neurons (Zheng *et al.*, 2008; Palmer *et al.*, 2009; Yadav *et al.*, 2012; Arthur *et al.*, 2015). Dual immunostaining for dynein and GM130 revealed increased colocalization of dynein and Golgi in DCX-deficient neurons compared with WT neurons (Figure 4, D and E). The increased colocalization may be a by-product of the increased Golgi localization in the soma, but not a direct effect of DCX. More experiments are needed to determine whether the changes in colocalization of dynein and Golgi complex influence somatic Golgi distribution in dendrites.

DCX deficiency significantly increased the colocalization of JIP3 and dynein

Various binding partners are known to regulate dynein functions (Vallee *et al.*, 2012). The interaction of DCX with dynein may alter the binding of regulatory proteins to the dynein motor complex to regulate dynein. We performed mass spectrometry (MS) experiments to identify proteins whose association with the dynein motor complex was altered in *Dcx-/y* brain lysates. DHC was immunoprecipitated from equal amounts of protein lysates from either WT or *Dcx-/y* P0 mouse brains using DHC-specific antibodies, followed by a proteomic analysis using MS. The identification of major subunits of dynein and dynactin revealed that our dynein coimmunoprecipitation experiments were successful (Table 2). Additionally, the absence of DCX altered the composition of the dynein motor complex and its association with various other proteins (Table 3). Consistent with our finding, DCX was among the proteins identified and its level was substantially diminished in the immunoprecipitate from the *DCX-/y* brain lysate (Table 3). Because mutations in either DCX or Lis1 both cause lissencephaly in humans, our initial hypothesis was that DCX changes Lis1 interactions with dynein. However, we did not detect Lis1 in our MS results. In contrast, we observed an eightfold increase in JIP3 binding to dynein in the absence of DCX (Table 3). JIP3 is an adaptor protein of kinesin and dynein that mediates both anterograde and retrograde transport (Arimoto *et al.*, 2011; Drerup and Nechiporuk, 2013). Immunostaining of both JIP3 and dynein also suggests that there is an increased JIP3 association with dynein in DCX-deficient neurons compared with WT (Figure 5A). Using Western blot analyses, we confirmed that the interaction of JIP3 with dynein (Figure 5, B and C) was increased in the absence of DCX, although the total JIP3 levels were similar in the presence

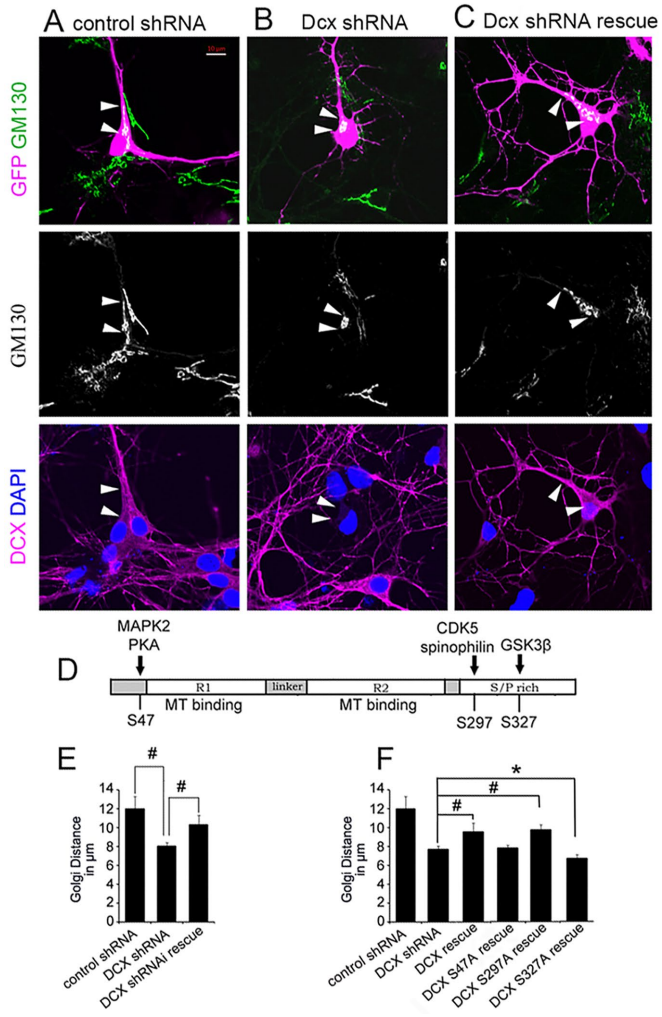

FIGURE 2: Rescue mediated by shRNA reveals the importance of DCX phosphorylation on Golgi outpost formation. (A) Cultured hippocampal cells from embryonic day 18 (E18) mice were transfected with vectors expressing GFP and a scrambled control shRNA (A); GFP and DCX shRNA (B); GFP, DCX shRNA, and full-length DCX tagged with HA (DCX shRNA rescue) on DIV 3 (C). Three days after transfection (DIV6), cells were immunostained for the Golgi (GM130) and DCX. Arrowheads indicate the location of the Golgi apparatus and the edge of the nucleus. The scale bar represents 10 μm. (D) The schematic of the rescue construct is shown with residues of interest for subsequent studies. (E) The distance of the Golgi to the nuclear envelope was measured and quantified in transfected neurons (n = 220, 198, 176 for control, Dcx shRNA, and Dcx rescue, respectively). The expression of full-length DCX in DCX-deficient neurons rescues the phenotype of impaired Golgi extension into dendrites. The scale bar represents 10 μm. (F) Plasmids expressing nonphosphorylatable DCX mutants S47A, S297A or S327A were cotransfected with plasmids expressing GFP and the DCX shRNA on DIV3, and cells were stained for GM130 on DIV6. Distances of somatic Golgi to the nucleus in each rescue experiment were measured and compared with cells transfected with the DCX shRNA. Both DCX and DCX S297A rescued the Golgi phenotype, but not DCX S327A and S47A. Furthermore, DCX S327A further decreased the distance of the somatic Golgi to the nucleus, suggesting a dominant negative effect. Data were obtained from three independent experiments, and more than 150 neurons (n = 220, 198, 176, 192, 159, and 210 for each group) were analyzed. $^{*}P < 0.05$, $^{\#}P < 0.01$, P values were calculated from t tests.

and absence of DCX (JIP3 levels in inputs, Figure 5B). We did not detect a direct interaction between JIP3 and DCX (data not shown).

The next question we asked was whether JIP3 was involved in the effects of DCX on the Golgi distribution in neurons. We used a plasmid overexpressing JIP3 to partially mimic the increased JIP3 colocalization with dynein observed in DCX-deficient neurons (Figure 5, B and C). Meanwhile, a bicistronic-GFP vector expressing a JIP3-specific shRNA was used to knock down JIP3 levels. The efficacy in JIP3 knockdown was validated in HEK293 cells overexpressing JIP3 (Figure 5D). Endogenous JIP3 levels in HEK293 cells (nonneuronal cells) were not detectable based on our observation, consistent with reports that JIP3 is mainly expressed in neurons (Arimoto *et al.*, 2011). Both JIP3 shRNA1 and shRNA2, but not shRNA3, significantly decreased JIP3 levels (Figure 5D). Although the introduction of JIP3 shRNA1 alone in WT neurons did not exert obvious effects on changing the Golgi distribution, down-regulation of JIP3 levels by JIP3 shRNA1 rescued the Golgi phenotype in DCX-deficient neurons, suggesting that JIP3 is required for DCX knockdown effects on somatic Golgi dendritic distribution. Compared to controls, JIP3 overexpression alone (JIP3 in Figure 5F) or in combination with DCX knockdown (JIP3+DCX KD in Figure 5F) significantly decreased the extension of the Golgi apparatus into dendrites (Figure 5, E and F). However, Golgi distance in the JIP3+DCX KD group is not significantly different from that in DCX KD alone or JIP3 alone, suggesting that JIP3 overexpression has similar but no synergistic effect with DCX shRNA to decrease cytoplasmic Golgi distribution. JIP3 overexpression alone decreased somatic Golgi extension, suggesting that JIP3 might have a DCX-independent effect on Golgi. Nevertheless, the evidence that JIP3 knockdown in DCX-deficient neurons but not in WT neurons rescued the Golgi phenotype supports that JIP3 is involved in DCX effects on somatic Golgi extension.

The N-terminal part (1–240) of *Caenorhabditis elegans* JIP3 has been reported to bind the cytoplasmic dynein light intermediate chain (Arimoto *et al.*, 2011). Meanwhile, this region of human JIP3 overlaps with the kinesin1 binding site and contains an RH1 (RILP homology 1) domain and LZ1 coiled-coil domain, which might link cytoskeletal motors and Rab GTPases (Vilela *et al.*, 2019). The N-terminal part of mouse JIP3 exhibits 98% similarity to human JIP3 (based on a BLAST alignment). Based on these reports, we developed a plasmid to express mouse JIP3 lacking the N-terminal region (1–240), serving as a JIP3 mutant (C-JIP3) without the ability to bind dynein. Indeed, C-JIP3 overexpression alone in WT (C-JIP3 in Figure 5F) lost effects on Golgi extension, similar to control and different from JIP3. This result suggests that the JIP3/dynein motor interaction is important for Golgi distribution. Compared to JIP3+DCX KD or DCX KD, overexpression of C-JIP3 combined with DCX knockdown (C-JIP3+DCX KD) reversed DCX KD effects. The results suggest that the interaction between JIP3 and dynein or other molecular motors is required for the role of JIP3 in the effects of DCX on the somatic Golgi distribution (Figure 5, E and F). It is interesting to notice that C-JIP3 effects (C-JIP3 and C-JIP3+DCX KD) on Golgi extension are similar to those of JIP3 knockdown (JIP3 KD and JIP3 KD+ DCX KD), implying that C-JIP3 might serve as dominant negative form of JIP3.

DISCUSSION

In the present study, the distribution of the somatic Golgi apparatus in dendrites was significantly decreased in DCX/DCLK1-deficient neurons. This defect is likely mediated by multiple factors working possibly both in parallel upstream and downstream of DCX/DCLK1. First, the regulation of MT binding and distribution of DCX by

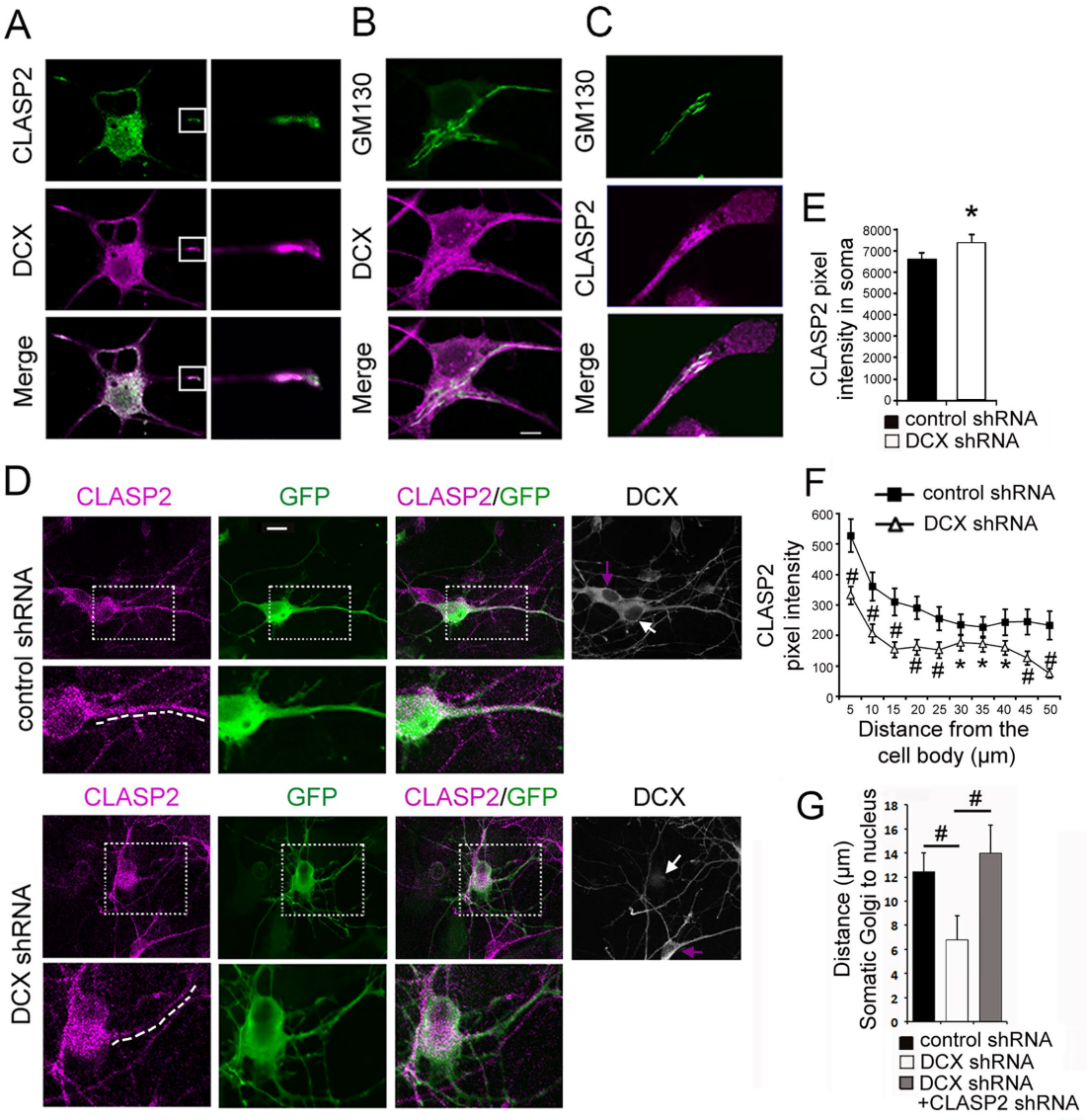

FIGURE 3: Loss of DCX decreases CLASP2 localization in dendrites. (A–C) Cultured WT hippocampal neurons were fixed on DIV5 and immunostained for DCX, CLASP2, and GM130, as indicated. (A) DCX and CLASP2 were distributed similarly in the neuronal soma and distal dendrites. (B) Dual immunostaining for DCX and GM130. (C) Dual immunostaining for DCLASP2 and GM130. (D) Cultured hippocampal neurons were transfected with plasmids expressing GFP and a control (scrambled) shRNA or DCX shRNA on DIV3. Transfected neurons were fixed on DIV6 and immunostained for DCX and CLASP2. GFP-positive cells were transfected with shRNA constructs that also express GFP. The CLASP2 intensity was quantified along the trajectories of neural processes starting from the soma and extending out 50 μm (shown as a broken white line adjacent to the neurite). White or purple arrows indicate DCX staining in transfected neurons or nontransfected neurons, respectively. (E) The intensity of CLASP2 immunostaining was measured in the soma of control or Dcx KD neurons. Significantly higher CLASP2 levels were detected in the soma of mutants ($n = 42$) than in controls ($n = 47$). (F) CLASP2 intensities in neural processes from control ($n = 47$) or DCX KD ($n = 42$) neurons were quantified from the soma and extending to 50 μm. (G) CLASP2 knockdown with CLASP2 shRNA-A rescued the Golgi phenotype observed in DCX-deficient neurons. The results were obtained from three independent experiments and 140 neurons from each condition. $^{\#}P < 0.01$, P values were calculated from the t test. The scale bar represents 10 μm.

phosphorylation of DCX at S47 and S327 may play roles in regulating the Golgi distribution. Second, the effects of DCX on CLASP2 modulate the effects. Finally, the influence of DCX to JIP3-dynein interaction is important for this process.

We propose a model to show the mechanism of DCX effects on somatic Golgi extension (Figure 6). In WT neurons, DCX promotes kinesin–3-mediated anterograde transports (Liu *et al.*, 2012). DCX binds dynein while inhibiting the association between JIP3 and dynein. Golgi moves along MTs toward their minus ends with the assistance of cytoplasmic dynein (Corthesy-Theulaz *et al.*, 1992; Fath *et al.*, 1994; Baas and Lin, 2010). We hypothesize that DCX negatively regulates dynein-mediated retrograde transports. The combination of DCX effects on retrograde transports and anterograde transports directly or indirectly contributes to somatic Golgi extension into dendrites. In DCX knockout (KO) neurons, more CLASP2 and kinesin-3 proteins are restricted within the area of

Purpose	Target	Targeted sequence
ShRNAi for DCX knockdown	DCX (NM_010025)	CGGTGTAATGTGCTCAGATAA
shRNAi1 for JIP3 knockdown	JIP3 (NM_013931)	GTCCGATGTTCAGGACATTA
shRNAi2 for JIP3 knockdown	JIP3 (NM_013931)	TGTTGTGAATGACCGAGTTTG
shRNAi3 for JIP3 knockdown	JIP3 (NM_013931)	AACAGGCCGAGGAGAAATTCA
shRNAi-A for CLASP2 knockdown	CLASP2 (NM_029633.2)	GCATCAGTCCTTTCAACAAGT
shRNAi-B for CLASP2 knockdown	CLASP2 (NM_029633.2)	GAACTTGAAGAGACGTTAAAT
Scrambled shRNAi for DCX	N/A	GGACTATTATGCGAGAGCTAT
Scrambled shRNAi for CLASP2	N/A	CCGCAGGTATGCACGCGTTAT
Universal control shRNAi	N/A	TTCTCCGAACGTGTCACGT

TABLE 1: The targeted sequences for shRNAi knockdown.

soma. Since CLASP2 is one of the effectors of the Reelin pathway, it would be interesting to determine whether the Reelin pathway played a role in DCX effects on Golgi extension. Kinesin–3-mediated anterograde transports are significantly decreased without DCX (Liu *et al*., 2012). Furthermore, without competition from DCX, more JIP3 molecules bind dynein with the help from an unknown adaptor protein. We hypothesize that dynein-mediated retrograde transports are increased when dynein is associated with JIP3 but not with DCX. The broken balance between anterograde transports and retrograde transports without DCX results in less Golgi extension into dendrites.

Cytoplasmic dynein and its cofactors play an important role in Golgi positioning (Yadav and Linstedt, 2011; Jaarsma and Hoogenraad, 2015). Dynein effects on Golgi in neurons are mainly based on studies using *Drosophila melanogaster*. The effects of dynein on the position of the Golgi complex in hippocampal and cortical neurons are unclear. In the present study, the colocalization of dynein with the Golgi in mouse neurons was significantly increased in the absence of DCX, implying that Golgi extension into dendrites may be sensitive to the amount of dynein associated with the Golgi apparatus. Future work is needed to approve this and clarify if the increased colocalization between dynein and Golgi complex is not a by-product of the increased Golgi localization in the soma. Since DCX is involved in kinesin–3-mediated transports (Liu *et al*., 2012), it is worthy to investigate whether DCX is involved in dynein-mediated retrograde transports, which might regulate the Golgi complex distribution. Moreover, the interaction of JIP3 with dynein was significantly increased in the absence of DCX. We propose that JIP3 and DCX have an opposite effect on Golgi dendritic extension. JIP3 overexpression decreased the distribution of the Golgi complex in dendrites because more JIP3 molecules are associated with dynein. A decrease in JIP3 levels mediated by the JIP3 shRNA has normal Golgi distribution because very few JIP3 binds dynein. This result is consistent with a report that no Golgi defects are observed in mouse neurons with JIP3 KO (Gowrishankar *et al*., 2017).

JIP3 colocalizes with DIC or DHC (Cavalli *et al*., 2005) and interacts with dynein subunits such as p150 (Cavalli *et al*., 2005). Somatic Golgi extension is normal in neurons expressing JIP3 mutant without N-terminal potential dynein binding domain, suggesting that the interaction between JIP3 and dynein or other molecular motors is required for the role of JIP3 in regulating the somatic Golgi distribution. A previous report showed that UNC-16 (JIP3 homologous protein in *C. elegans*) needs adaptor protein kinesin-1 to be associated with dynein (Arimoto *et al*., 2011). We propose that JIP3 in mouse neuron also needs the help from an adaptor protein to bind dynein. This adaptor binds JIP3 through a different domain (not the N-terminal dynein binding domain) of JIP3. When C-JIP3 is overexpressed in DCX KO neurons, the adaptor protein is saturated with C-JIP3 and then very few JIP3 can bind dynein, a phenomenon similar to that observed in WT neurons. This explains why C-JIP3 overexpression can rescue the Golgi phenotype in DCX KO neurons. To identify this unknown adaptor protein in the future will be very helpful to support our results and hypothesis. Meanwhile, JIP3 overexpression alone can decrease somatic Golgi extension, and it is still possible that JIP3 has DCX-independent effects on Golgi extension.

JIP3 in *C. elegans* seems to have stronger effects to regulate the transport of the Golgi and to inhibit Golgi positioning beyond the axon initial segment (Edwards *et al*., 2013, 2015). The Golgi apparatus accumulates to a 10-fold higher level in UNC-16-deficient axons than in WT axons (Edwards *et al*., 2013). A possible explanation is that there exists other proteins with compensating function for JIP3 to control the Golgi distribution in mammalian neurons but not in *C. elegans*. In addition, JIP3 is a multifunctional protein involved in multiple trafficking pathways. JIP3 regulates synaptic vesicle protein trafficking from the Golgi complex by recruiting effectors such as LRK-1 (Choudhary *et al*., 2017; Gowrishankar *et al*., 2017). JIP3 interacts dynein through kinesin-1, which is involved in both anterograde and retrograde axonal transport (Arimoto *et al*., 2011; Sun *et al*., 2011). UNC-16 also interacts with kinesin-3, and their interaction changes the kinesin-3 location in *C. elegans* neurons (Hsu *et al*., 2011). To determine whether kinesin-3 interacts with JIP3 to regulate Golgi extension will be interesting to further understand the underline mechanism. As shown in our previous study, DCX/DCLK1 deficiency decreases the overall neurite length and increases the number of primary neurites directly arising from the soma (Liu *et al*., 2012). In mammalian neurons, the somatic Golgi apparatus extends into the longest or apical dendrite, while it is not observed to polarize toward the axon (Krijnse-Locker *et al*., 1995; Horton and Ehlers, 2003; Horton *et al*., 2005; Ye *et al*., 2007). Our observation is consistent with these reports. One unique difference between axons and dendrites is that MT polarity in dendrites is mixed, whereas the MTs in axons are uniformly oriented with their plus-ends positioned distal to the cell body, which might contribute to the absence of the Golgi apparatus in axons, since the Golgi is known to move along MTs toward their minus ends with the assistance of cytoplasmic dynein (Corthesy-Theulaz *et al*., 1992; Fath *et al*., 1994; Baas and Lin, 2010). Various studies have defined an important role for the Golgi complex in the development of both axons and dendrites and the maintenance of the highly polarized morphology of neurons (Horton and Ehlers, 2003; Horton *et al*., 2005; Ye *et al*., 2007;

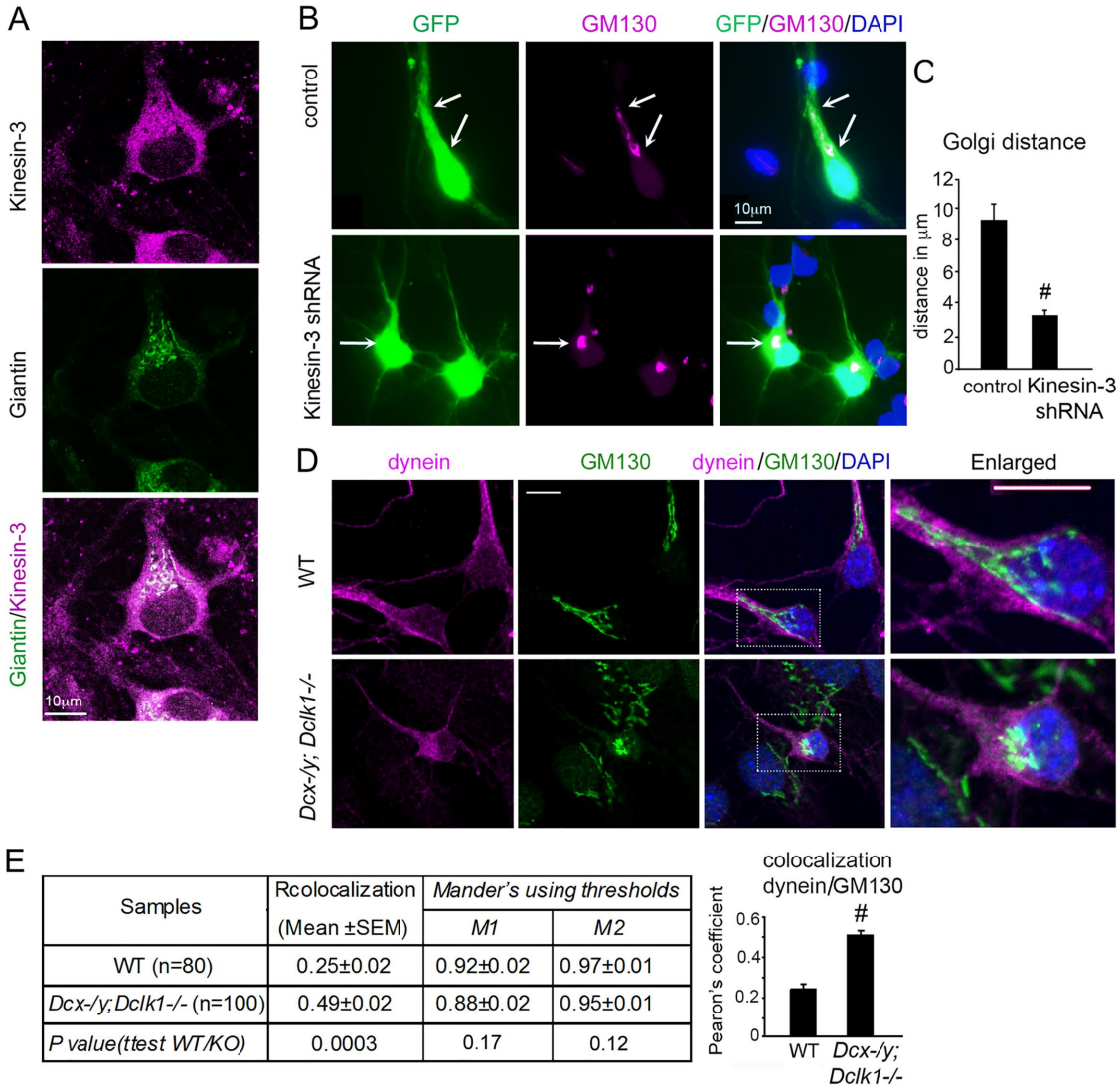

E

Samples	Rcolocalization (Mean ±SEM)	*Mander's using thresholds*	
		M1	*M2*
WT (n=80)	0.25±0.02	0.92±0.02	0.97±0.01
Dcx-/y;Dclk1-/- (n=100)	0.49±0.02	0.88±0.02	0.95±0.01
P value(ttest WT/KO)	0.0003	0.17	0.12

FIGURE 4: Molecular motors and the somatic Golgi dendritic distribution (A) Cultured WT hippocampal neurons (DIV5) were stained with the Golgi marker giantin and kinesin-3. (B) Down-regulation of kinesin-3 with the kinesin-3 shRNA decreased the dendritic distribution of the Golgi compared with the control. Arrows indicate the locations of Golgi stained with GM130. (C) The distances of the somatic Golgi to the nucleus were quantified and compared. Data were obtained from three independent experiments, and 90 neurons were analyzed from each condition. (D) Cultured hippocampal neurons (DIV5) from WT or *Dcx-/y; Dclk1–/–* mice were stained with GM130 and DHC antibodies. (E) The colocalization between dynein and GM130 in cultured neurons from WT or *Dcx-/y; Dclk1–/–* was calculated using the "Colocalization Threshold" plugin of the ImageJ software platform. Only GM130-stained regions were outlined and analyzed for colocalization. Pearson's correlation coefficient (Rcolocalization) and Mander's colocalization coefficient (M1 and M2) calculated from the analysis are shown in the table. Rcolocalization is defined as Pearson's correlation coefficient for pixels where both the red channel (dynein) and green channel (GM130) are above their respective thresholds. M1 and M2 are Mander's colocalization coefficients obtained using thresholds. Data are based on three independent experiments from each condition. *P* values were calculated from *t* tests. $^{*}P < 0.05$, $^{\#}P < 0.01$. Scale bars represent 10 μm.

Ori-McKenney *et al.*, 2012; Zhou *et al.*, 2014; Rao *et al.*, 2018; Yang and Wildonger, 2020). Therefore, the decrease in somatic Golgi extension into dendrites might contribute to the morphological defects observed in DCX/DCLK1-deficient neurons.

Both CLASP2 and DCX partially colocalize with the Golgi apparatus. In DCX/DCLK1-deficient neurons, more CLASP2 proteins are located in the soma than in dendrites compared with WT neurons. CLASP2 is a MT plus-end tracking protein that promotes MT growth from the Golgi apparatus (Mimori-Kiyosue *et al.*, 2005; Miller *et al.*, 2009). CLASP2 is asymmetrically distributed in neurons and usually accumulates at the end of neurites close to the growing plus-ends of the MT (Akhmanova *et al.*, 2001; Wittmann and Waterman-Storer, 2005), similar to the distribution of DCX in neurons. CLASP2 also regulates the Golgi morphology (Miller *et al.*, 2009; Beffert *et al.*, 2012; Dillon *et al.*, 2017). In cultured hippocampal neurons, CLASP2 overexpression increases the stacking of Golgi apparatuses in the soma and reduces their deployment into dendrites (Beffert *et al.*, 2012). In DCX/DCLK1-deficient neurons, we observed greater

Id	Sequence name	Dcx KO	WT	K/W
Q9JHU4	DYHC1 Cytoplasmic dynein 1 heavy chain 1	30.1	54	0.56
Q9D0M5	DYL2 Dynein light chain 2, cytoplasmic	15.05	12	1.25
P63168	DYL1 Dynein light chain 1, cytoplasmic	17.37	11	1.58
P62627	DLRB1 Dynein light chain roadblock-type 1	3.47	5	0.69
Q8R1Q8	DC1L1 Cytoplasmic dynein 1 light intermediate chain 1	2.32	5	0.46
O88487	DC1I2 Cytoplasmic dynein 1 intermediate chain 2	0	3	0.00
O08788	DCTN1 Dynactin subunit 1	5.79	5	1.16
Q99KJ8	DCTN2 Dynactin subunit 2	3.47	4	0.87
Q9Z0Y1	DCTN3 Dynactin subunit 3	3.47	2	1.74

TABLE 2: Subunits of dynein and dynactin identified by MS.

somatic localization of CLASP2, which likely mimics the somatic condition of cells overexpressing CLASP2 and then contributes to an increase in the number of Golgi apparatuses stacked in the neuronal soma. CLASP2 is the downstream effector of the Reelin pathway that connects with the cytoskeleton system to influence neuronal migration (Dillon *et al.*, 2017). Meanwhile, the Reelin pathway is known for its functions in neuronal migration (D'Arcangelo *et al.*, 1995). Similar to the DCX gene, both RELN and its receptor VLDLR are causative genes for lissencephaly (Hong *et al.*, 2000; Di Donato *et al.*, 2018). Based on our data, CLASP2 is a downstream effector of DCX. Therefore, CLASP2 may connect the Reelin signaling pathway to DCX.

DCX is known to be regulated by phosphorylation at different Ser/Thr sites. Researchers have proposed that phosphorylation–dephosphorylation cycles at specific DCX sites may serve as a molecular switch determining the cellular location and function of DCX (Schaar *et al.*, 2004; Shmueli *et al.*, 2006). Several pathways are involved, including CDK5 (Graham *et al.*, 2004; Tanaka *et al.*, 2004b), Rho kinase (Amano *et al.*, 2010), MAPK2 and PKA (Schaar *et al.*, 2004), JNK (Gdalyahu *et al.*, 2004), and GSK3-β (Bilimoria *et al.*, 2010). Conversely, phosphatase I dephosphorylates DCX (Shmueli *et al.*, 2006; Bielas *et al.*, 2007). In the present study, the phosphorylation-resistant DCX mutants S47A and S327A did not rescue the Golgi phenotype in DCX-deficient neurons, suggesting that phosphorylation of DCX at S47 or S327 is important for promoting the elongation of somatic Golgi in dendrites. MAPK2 and PKA are responsible for the phosphorylation of DCX on S47 (Schaar *et al.*, 2004). The dephosphorylation of DCX at S47 results in a higher affinity for MTs, while DCX phosphorylated at S47 has a higher affinity for F-actin and is mainly located at actin-rich growth cones (Tsukada *et al.*, 2003, 2005; Gdalyahu *et al.*, 2004; Schaar *et al.*, 2004; Tanaka *et al.*, 2004b; Bielas *et al.*, 2007). JIP3 regulates GSK3-β, which specifically phosphorylates DCX on S327 (Bilimoria *et al.*, 2010). Here, DCX regulated the interaction of JIP3 with dynein. If the interaction of JIP3 with dynein modified JIP3 functions, such as its effects on GSK3-β, then a feedback loop might exist among JIP3, GSK3-β, and DCX. Furthermore, GSK3-β also phosphorylates CLASP2 to control cell motility and neurite extension (Dillon *et al.*, 2017). GSK3-β might be a critical factor influencing the Golgi distribution in neurons and the missing link connecting JIP3, DCX, and CLASP2. A further examination of the role of GSK3-β in regulating Golgi distribution in neurons is required in the future.

In summary, we identified CLASP2, dynein, and JIP3 as new targets of DCX that are likely involved in the effects of DCX on the dendritic distribution of the somatic Golgi apparatus in mouse neurons. The Reelin or GSK3-β pathway might also involve in this process. Our study also suggests a possible new functional interaction among DCX, JIP3, and dynein. Further investigations of whether DCX exerts potential effects on other functions of dynein, such as retrograde transport, are needed. Our study provides new insights into the role of DCX in neuronal development and migration.

MATERIALS AND METHODS

Antibodies and reagents

Cell culture reagents, including Lipofectamine 2000 that was used for transfection, were purchased from Thermo Fisher Scientific (Waltham, MA). Antibodies against DCX (ab18723), DHC (ab6305), GM130 (ab169276, ab52649), JIP3 (ab196761), and DIC (ab23905) were purchased from Abcam (Cambridge, MA). Antibodies against CLASP2 were obtained from Santa Cruz (sc-376496, Dallas, TX) or Novus Biologicals (NBP1-21394, Centennial, CO). Antibodies against HA were obtained from EMD Millipore (Billerica, MA).

Mammalian expression and RNA interference constructs

HA-tagged (N-terminus) DCX mutants were created using a QuikChange Site-Directed Mutagenesis kit (Stratagene). The target sequences included in shRNAs to silence the expression of mouse DCX, JIP3, or CLASP2 are indicated in Table 1. The corresponding scrambled sequences are also shown in Table 1. The complementary RNAi oligos were annealed and ligated into pSilencer-GFP (gift from Shirin Bonni), which is a bicistronic plasmid that coexpresses the shRNA and eGFP, as previously described by Konishi *et al.* (Konishi *et al.*, 2004; Sarker *et al.*, 2005).

Animals, primary neuronal cultures, and immunostaining

All animal procedures were approved by the Committee on the Ethics of Animal Experiments of Wenzhou Medical University. On embryonic day (E) 15 cortices or E17.5 hippocampi were dissected and dissociated using the Worthington papain dissociation system (LK003150, Worthington Biochemical). Neurons were plated on polyornithine-coated (Sigma) cover glasses in neuronal culture medium (Neurobasal medium plus B27, glutamine, FGF [10 μg/ml], and Pen/Strep) until use in the experiments. Cells were fixed with 4% paraformaldehyde, immunostained with standard techniques, and counterstained with the nuclear dye DAPI (Invitrogen). The images were acquired using a Zeiss LSM510 line-scanning confocal microscope or a Zeiss AxioVert A1 fluorescence microscope. Images of samples from the same experiment were acquired and analyzed using the same acquisition and processing parameters,

Id	Sequence name	Dcx KO	WT	K/W
O88809	DCX	1.16	81	0.01
Q61553	Fascin	1.16	51	0.02
Q8K0E8	Fibrinogen beta chain	2.32	30	0.08
P30999	Catenin delta-1	1.16	9	0.13
Q6PGN3	DCLK2	4.63	32	0.14
Q6PDG5	SWI/SNF complex subunit SMARCC2	2.32	15	0.15
Q8VCM7	Fibrinogen gamma chain	3.47	22	0.16
Q6PIC6	Sodium/potassium-transporting ATPase subunit alpha-3	5.79	29	0.2
Q9CQZ1	Heat shock factor-binding protein 1	2.32	11	0.21
O70152	Dolichol-phosphate mannosyltransferase	1.16	4	0.29
Q9D1C8	Vacuolar protein sorting-associated protein 28 homolog	1.16	4	0.29
Q9EQH3	Vacuolar protein sorting-associated protein 35	1.16	4	0.29
Q9QYB8	Beta-adducin	2.32	8	0.29
O54962	Barrier-to-autointegration factor	2.32	8	0.29
Q9QWI6	SRC kinase signaling inhibitor 1	8.1	28	0.29
Q91Z31	Polypyrimidine tract-binding protein 2	3.47	11	0.32
Q9EPN1	Neurobeachin	2.32	7	0.33
P97450	ATP synthase-coupling factor 6, mitochondrial	3.47	10	0.35
P26040	Ezrin	3.47	9	0.39
Q8K3G9	DCC-interacting protein 13-beta	6.95	18	0.39
O70133	ATP-dependent RNA helicase A	17.37	44	0.39
Q501J6	Probable ATP-dependent RNA helicase DDX17	11.58	29	0.4
P02089	Hemoglobin subunit beta-2	31.26	78	0.4
Q08509	Epidermal growth factor receptor kinase substrate 8	3.47	8	0.43
Q0KL02	Triple functional domain protein	3.47	8	0.43
Q8K310	Matrin-3	33.58	78	0.43
Q99P72	Reticulon-4	5.79	13	0.45
P26231	Catenin alpha-1	2.32	5	0.46
Q8R1Q8	Cytoplasmic dynein 1 light intermediate chain 1	2.32	5	0.46
Q61166	MT-associated protein RP/EB family member 1	2.32	5	0.46
Q9QXS1	Plectin	28.94	63	0.46
Q9WV69	Dematin	12.74	26	0.49
O88398	Advillin	15.05	31	0.49
Q9JLM8	DCLK1	46.31	69	0.67
P02088	Hemoglobin subunit beta-1	50.94	104	0.49
Q8BG95	Protein phosphatase 1 regulatory subunit 12B	8.1	4	2.03
Q99MK8	Beta-adrenergic receptor kinase 1	4.63	2	2.32
Q3TGF2	Protein FAM107B	4.63	2	2.32
Q3TTY5	Keratin, type II cytoskeletal 2 epidermal	16.21	7	2.32
Q5PR69	Uncharacterized protein KIAA1211	24.31	10	2.43
P57746	V-type proton ATPase subunit D	8.1	3	2.70
P51880	Fatty acid-binding protein, brain	5.79	2	2.90
Q01405	Protein transport protein Sec23A	5.79	2	2.90
Q3UQA7	Selenoprotein H	5.79	2	2.90
P56480	ATP synthase subunit beta, mitochondrial	11.58	4	2.90
Q9WUM4	Coronin-1C	18.52	6	3.09
P01837	kappa chain C region	16.21	4	4.05
P11031	Activated RNA polymerase II transcriptional coactivator p15	4.63	1	4.63
P03987	Ig gamma-3 chain C region	18.52	4	4.63
Q8BTM8	Filamin-A	16.21	3	5.40
P48453	Serine/threonine-protein phosphatase 2B catalytic subunit beta isoform	20.84	3	6.95
Q9ESN9	JIP3 C-Jun-amino-terminal kinase-interacting protein 3	17.37	2	8.69

TABLE 3: Comparison of MS results of WT and *Dcx-/y* showing different protein distributions. More JIP3 bound to DHC without DCX, as determined by spectral counts. DCX is confirmed as a DHC binding protein.

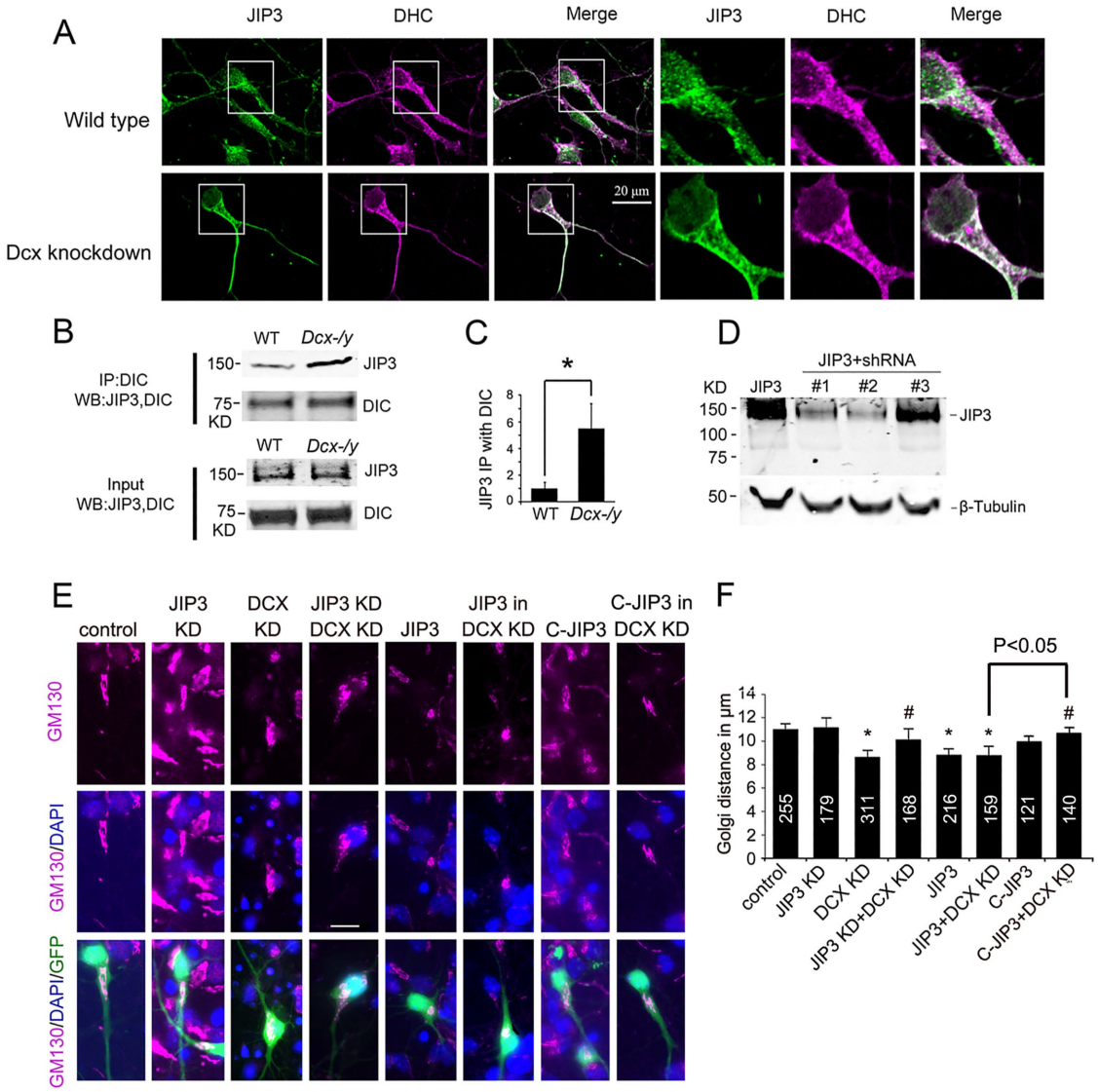

FIGURE 5: The dynein cofactor JIP3 is involved in the effects of DCX on the dendritic distribution of the Golgi. (A) Immunostaining for JIP3 and DHC in cultured neurons from WT and *Dcx-/y* P0 mice on DIV5. (B) Immunoprecipitation of DIC and Western blot showing JIP3 levels in protein lysates from P0 WT or *Dcx-/y* mouse brains. (C) Quantification of Western blot bands for JIP3 pulled down with a DIC antibody normalized to JIP3 inputs. The results were obtained from three independent experiments. (D) Three JIP3 shRNAs were validated for their ability to down-regulate JIP3 expression. Different groups of HEK293 cells were transfected with a plasmid overexpressing JIP3 (lane 1) or plasmid overexpressing JIP3 and plasmid expressing one of the three JIP3 shRNAs (lanes 2–4). (E) Representative images showing the effects of JIP3 on the somatic Golgi (GM130) distribution. Cultured neurons were transfected with different plasmids to modify gene expression: control (control shRNA), JIP3 KD (JIP3 shRNA#1), DCX KD (DCX shRNA), JIP3 (overexpressing JIP3), C-JIP3 (overexpressing C-JIP3), or their combinations on DIV4. The dendritic distribution of the Golgi apparatus was observed by performing GM130 immunostaining on DIV 6. Scale bars represent 10 μm. (F) The distances from the Golgi to the nuclear envelope were measured and analyzed for cells from each condition. Data were obtained from three independent experiments. The number of neurons analyzed in each group is shown in each bar. $^{*}P < 0.05$, compared with control group; $^{\#}P < 0.05$, compared with DCX KD group, *P* values were calculated from *t* tests.

such as the same exposures and background subtraction. All image analyses were blindly assigned to observers to avoid unconscious bias.

Measuring the distance from the somatic Golgi apparatus to the nucleus

The distance from the somatic Golgi apparatus to the nucleus was measured from the distal edge of the somatic Golgi apparatus to the closest edge of the nucleus. A schematic of the measurement procedure is shown in Figure 1B.

Measurement of CLASP2 immunostaining intensity in dendrites

To measure CLASP2 intensity in dendrites, segmented line in ImageJ was used to outline the dendrite to be measured and the width was adjusted based on each dendrite. The outlined dendrite

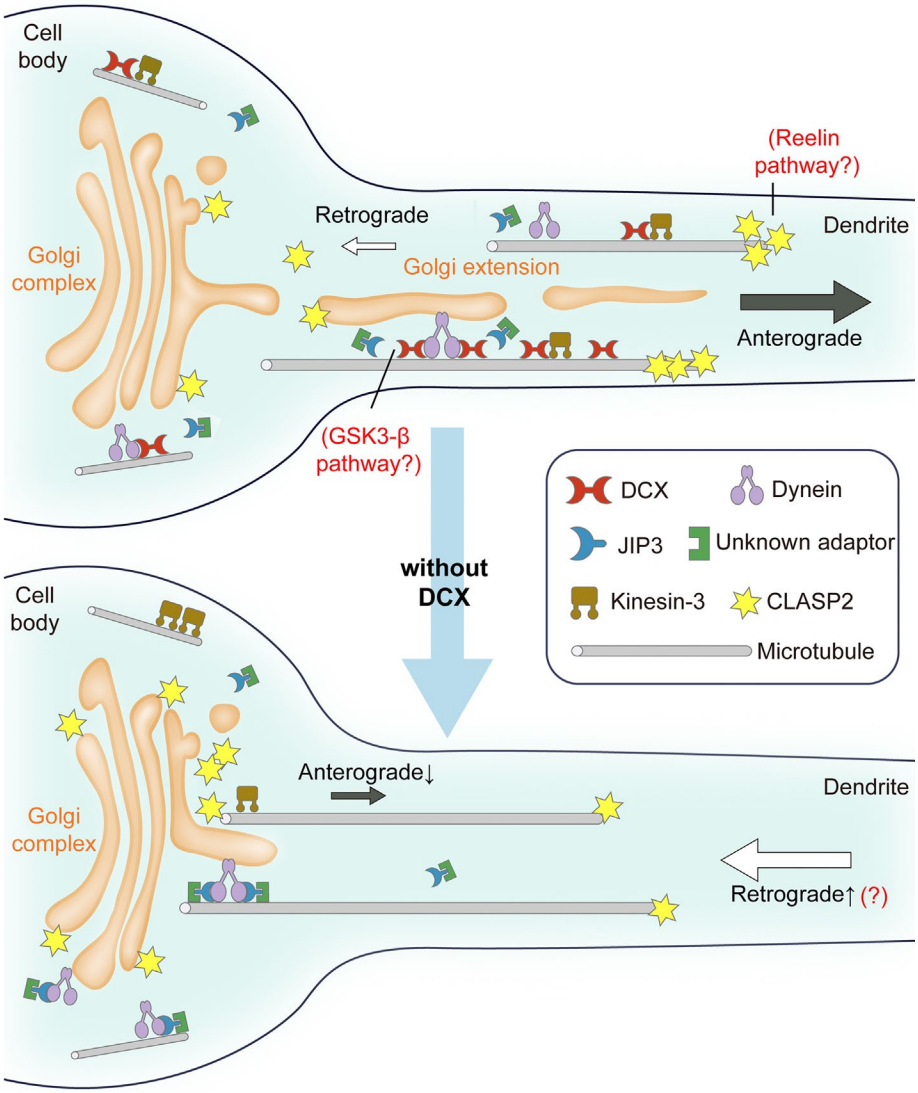

FIGURE 6: Schematic diagram shows that DCX facilitates the extension of the somatic Golgi complex into dendrite through MT-associated proteins and motors. In WT neurons, DCX association with kinesin-3 helps kinesin–3-mediated anterograde transports (Liu *et al.*, 2012). Meanwhile, DCX binds dynein while inhibiting JIP3. We hypothesize that DCX negatively regulates dynein-mediated retrograde transports. The combination of DCX effects on retrograde and anterograde transports guarantee the normal extension of somatic Golgi complex into dendrites. In DCX KO neurons (without DCX), more CLASP2 and kinesin-3 proteins are restricted in neuronal soma. Kinesin–3-mediated anterograde transports are decreased without DCX (Liu *et al.*, 2012). More JIP3 molecules bind dynein. JIP3 needs to bind an adaptor protein before associates with dynein. We hypothesize that dynein-mediated retrograde transports are increased with JIP3 association while not bound with DCX. The balance between anterograde transports and retrograde transports is changed without DCX, which results in less Golgi extension into dendrites.

was straightened using Straighten function, from which a new image was created and saved. From the created image, the intensity of CLASP2 along the dendrite is measured using ImageJ's integrated density measurement.

Quantification of colocalization

Colocalization of two colors in dual immunostaining images was analyzed using the ImageJ plug Colocalization Threshold in the ImageJ analysis software platform. Each GM130-positive region in an image with both GM130 and dynein immunostaining was outlined, saved as a new file, and used to analyze the colocalization of GM130 and dynein. Rcolocalization from the analysis is Pearson's correlation coefficient for pixels where both the red channel (dynein) and the green channel (GM130) are above their respective threshold. M1 and M2 are Mander's colocalization coefficients calculated using thresholds. Pearson's correlation coefficient was quantified as a number ranging from –1 and +1. A value of 0 for R indicates no correlation. A positive R indicates a positive correlation, and 1 indicates a complete or perfect correlation. A negative R indicates that the variables are inversely correlated. The strength of the correlation increases from 0 to +1 and from 0 to –1. M1 and M2 were quantified from 0 to 1, where 0 corresponds to nonoverlapping images and 1 reflects 100% colocalization between both images.

Western blot analysis

Standard Western blot analyses were performed as previously reported (Fu *et al.*, 2010). The dual channel signal detection Li-Cor system from Odyssey was used to analyze levels over a linear dynamic range.

MS procedure and analysis

Proteins extracted from three WT or *Dcx-/y* P0 mouse brains were precleared with normal serum and then processed through a standard immunoprecipitation protocol using anti-DHC antibodies and Protein A–conjugated beads. Mass spectra were searched against the UniProt mouse database (UniProt release-2010_11;16,333 entries) indexed for complete tryptic digestion, a 300–4000 mass range, and two missed cleavages using the SEQUEST algorithm in the BioWorks software package, version 3.2 (ThermoFinnigan). Mass tolerances were set to a 50 ppm error for MS and 1 Da error for MS/MS and the potential modification of oxidized methionine (15.99492 Da). Search results were uploaded to ProteoIQ label-free software, version 2.3.02, (www.bioinquire.com) for each sample, grouped in triplicate, and filtered as follows: 0.98 peptide probability, 0.95 protein probability, XCorr_1.9, four spectra, and two unique peptides for each protein. Scan counts were normalized based on the total sample intensity. Protein fold change values were calculated as the ratio of scan counts for each sample to its paired control. Protein annotations were acquired using http://www.uniprot.org/ (Fu *et al.*, 2013).

Transmission electron microscopy

Animals were intracardially perfused with 2.5% (vol/vol) glutaraldehyde and 2% (vol/vol) paraformaldehyde in phosphate-buffered saline, and then the brains were postfixed overnight in the same fixative. The brains were rinsed and dehydrated through a graded

series of ethanol solutions (50 to 100% ethanol) and embedded in Durcupan resin (Sigma). Ultrathin sections (70 nm) were collected on pioloform-coated EM copper grids (Agar Scientific) and stained with lead citrate. The sections were examined using a transmission electron microscope (TEM, H-600IV; HITACHI, Tokyo, Japan).

Western analysis

Standard Western analysis was performed as reported before (Fu *et al.*, 2010). The dual channel signal detection Odyssey system from Li-Cor was used to analyze levels over a linear dynamic range.

Statistical analysis

Statistical analyses were performed using GraphPad Prism 7.0 software (GraphPad Software, San Diego, CA). All data are presented as the mean ± SEM of at least three independent experiments. Statistical significance was determined using one-way analysis of variance (ANOVA) followed by Tukey's test if more than two groups were analyzed. Two-tailed test and Student's *t* test were used to compare two groups. $P < 0.05$ was considered significant ($*p < 0.05$; $\#p < 0.01$, if not specified otherwise).

ACKNOWLEDGMENTS

This study was supported by grants from the National Natural Science Funding of China (81971425 and 81871035), the Zhejiang Provincial Natural Science Foundation of China (LY20H040002 and LZ09H090001) and Wenzhou Basic Scientific Research project (Y20190001).

REFERENCES

Akhmanova A, Hoogenraad CC, Drabek K, Stepanova T, Dortland B, Verkerk T, Vermeulen W, Burgering BM, De Zeeuw CI, Grosveld F, *et al.* (2001). Clasps are CLIP-115 and -170 associating proteins involved in the regional regulation of microtubule dynamics in motile fibroblasts. Cell 104, 923–935.

Akhmanova A, Severin F (2004). Thirteen is the lucky number for doublecortin. Dev Cell 7, 5–6.

Amano M, Tsumura Y, Taki K, Harada H, Mori K, Nishioka T, Kato K, Suzuki T, Nishioka Y, Iwamatsu A, *et al.* (2010). A proteomic approach for comprehensively screening substrates of protein kinases such as Rho-kinase. PLoS One 5, e8704.

Arimoto M, Koushika SP, Choudhary BC, Li C, Matsumoto K, Hisamoto N (2011). The Caenorhabditis elegans JIP3 protein UNC-16 functions as an adaptor to link kinesin-1 with cytoplasmic dynein. J Neurosci 31, 2216–2224.

Arthur AL, Yang SZ, Abellaneda AM, Wildonger J (2015). Dendrite arborization requires the dynein cofactor NudE. J Cell Sci 128, 2191–2201.

Baas PW, Lin S (2010). Hooks and comets: The story of microtubule polarity orientation in the neuron. Dev Neurobiol 71, 403–418.

Beffert U, Dillon GM, Sullivan JM, Stuart CE, Gilbert JP, Kambouris JA, Ho A (2012). Microtubule plus-end tracking protein CLASP2 regulates neuronal polarity and synaptic function. J Neurosci 32, 13906–13916.

Bielas SL, Serneo FF, Chechlacz M, Deerinck TJ, Perkins GA, Allen PB, Ellisman MH, Gleeson JG (2007). Spinophilin facilitates dephosphorylation of doublecortin by PP1 to mediate microtubule bundling at the axonal wrist. Cell 129, 579–591.

Bilimoria PM, de la Torre-Ubieta L, Ikeuchi Y, Becker EB, Reiner O, Bonni A (2010). A JIP3-Regulated GSK3β/DCX signaling pathway restricts axon branching. J Neurosci 30, 16766–16776.

Cavalli V, Kujala P, Klumperman J, Goldstein LS (2005). Sunday Driver links axonal transport to damage signaling. J Cell Biol 168, 775–787.

Choudhary B, Kamak M, Ratnakaran N, Kumar J, Awasthi A, Li C, Nguyen K, Matsumoto K, Hisamoto N, Koushika SP (2017). UNC-16/JIP3 regulates early events in synaptic vesicle protein trafficking via LRK-1/LRRK2 and AP complexes. PLoS Genet 13, e1007100.

Corthesy-Theulaz I, Pauloin A, Pfeffer SR (1992). Cytoplasmic dynein participates in the centrosomal localization of the Golgi complex. J Cell Biol 118, 1333–1345.

D'Arcangelo G, Miao GG, Chen SC, Soares HD, Morgan JI, Curran T (1995). A protein related to extracellular matrix proteins deleted in the mouse mutant reeler. Nature 374, 719–723.

des Portes V, Pinard JM, Billuart P, Vinet MC, Koulakoff A, Carrie A, Gelot A, Dupuis E, Motte J, Berwald-Netter Y, *et al.* (1998). A novel CNS gene required for neuronal migration and involved in X-linked subcortical laminar heterotopia and lissencephaly syndrome. Cell 92, 51–61.

Deuel TA, Liu JS, Corbo JC, Yoo SY, Rorke-Adams LB, Walsh CA (2006). Genetic interactions between doublecortin and doublecortin-like kinase in neuronal migration and axon outgrowth. Neuron 49, 41–53.

Di Donato N, Timms AE, Aldinger KA, Mirzaa GM, Bennett JT, Collins S, Olds C, Mei D, Chiari S, Carvill G, *et al.* (2018). Analysis of 17 genes detects mutations in 81% of 811 patients with lissencephaly. Genet Med 20, 1354–1364.

Dillon GM, Tyler WA, Omuro KC, Kambouris J, Tyminski C, Henry S, Haydar TF, Beffert U, Ho A (2017). CLASP2 links Reelin to the cytoskeleton during neocortical development. Neuron 93, 1344–1358.e1345.

Drerup CM, Nechiporuk AV (2013). JNK-interacting protein 3 mediates the retrograde transport of activated c-Jun N-terminal kinase and lysosomes. PLoS Genet 9, e1003303.

Edwards SL, Morrison LM, Yorks RM, Hoover CM, Boominathan S, Miller KG (2015). UNC-16 (JIP3) Acts through synapse-assembly proteins to inhibit the active transport of cell soma organelles to *Caenorhabditis elegans* motor neuron axons. Genetics 201, 117–141.

Edwards SL, Yu SC, Hoover CM, Phillips BC, Richmond JE, Miller KG (2013). An organelle gatekeeper function for Caenorhabditis elegans UNC-16 (JIP3) at the axon initial segment. Genetics 194, 143–161.

Fath KR, Trimbur GM, Burgess DR (1994). Molecular motors are differentially distributed on Golgi membranes from polarized epithelial cells. J Cell Biol 126, 661–675.

Fu X, Brown KJ, Yap CC, Winckler B, Jaiswal JK, Liu JS (2013). Doublecortin (Dcx) family proteins regulate filamentous actin structure in developing neurons. J Neurosci 33, 709–721.

Fu X, Zang K, Zhou Z, Reichardt LF, Xu B (2010). Retrograde neurotrophic signaling requires a protein interacting with receptor tyrosine kinases via C2H2 zinc fingers. Mol Biol Cell 21, 36–49.

Gdalyahu A, Ghosh I, Levy T, Sapir T, Sapoznik S, Fishler Y, Azoulai D, Reiner O (2004). DCX, a new mediator of the JNK pathway. EMBO J 23, 823–832.

Gleeson JG, Allen KM, Fox JW, Lamperti ED, Berkovic S, Scheffer I, Cooper EC, Dobyns WB, Minnerath SR, Ross ME, *et al.* (1998). Doublecortin, a brain-specific gene mutated in human X-linked lissencephaly and double cortex syndrome, encodes a putative signaling protein. Cell 92, 63–72.

Gowrishankar S, Wu Y, Ferguson SM (2017). Impaired JIP3-dependent axonal lysosome transport promotes amyloid plaque pathology. J Cell Biol 216, 3291–3305.

Graham ME, Ruma-Haynes P, Capes-Davis AG, Dunn JM, Tan TC, Valova VA, Robinson PJ, Jeffrey PL (2004). Multisite phosphorylation of doublecortin by cyclin-dependent kinase 5. Biochem J 381, 471–481.

Guardia CM, Farias GG, Jia R, Pu J, Bonifacino JS (2016). BORC functions upstream of kinesins 1 and 3 to coordinate regional movement of lysosomes along different microtubule tracks. Cell Rep 17, 1950–1961.

Hendricks AG, Perlson E, Ross JL, Schroeder HW, 3rd, Tokito M, Holzbaur EL (2010). Motor coordination via a tug-of-war mechanism drives bidirectional vesicle transport. Curr Biol 20, 697–702.

Hong SE, Shugart YY, Huang DT, Shahwan SA, Grant PE, Hourihane JO, Martin ND, Walsh CA (2000). Autosomal recessive lissencephaly with cerebellar hypoplasia is associated with human RELN mutations. Nat Genet 26, 93–96.

Horesh D, Sapir T, Francis F, Wolf SG, Caspi M, Elbaum M, Chelly J, Reiner O (1999). Doublecortin, a stabilizer of microtubules. Hum Mol Genet 8, 1599–1610.

Horton AC, Ehlers MD (2003). Dual modes of endoplasmic reticulum-to-Golgi transport in dendrites revealed by live-cell imaging. J Neurosci 23, 6188–6199.

Horton AC, Racz B, Monson EE, Lin AL, Weinberg RJ, Ehlers MD (2005). Polarized secretory trafficking directs cargo for asymmetric dendrite growth and morphogenesis. Neuron 48, 757–771.

Hsu CC, Moncaleano JD, Wagner OI (2011). Sub-cellular distribution of UNC-104(KIF1A) upon binding to adaptors as UNC-16(JIP3), DNC-1(DCTN1/Glued) and SYD-2(Liprin-alpha) in C. elegans neurons. Neuroscience 176, 39–52.

Jaarsma D, Hoogenraad CC (2015). Cytoplasmic dynein and its regulatory proteins in Golgi pathology in nervous system disorders. Front Neurosci 9, 397.

Kaplan A, Reiner O (2011). Linking cytoplasmic dynein and transport of Rab8 vesicles to the midbody during cytokinesis by the doublecortin domain-containing 5 protein. J Cell Sci 124, 3989–4000.
Keays DA, Tian G, Poirier K, Huang GJ, Siebold C, Cleak J, Oliver PL, Fray M, Harvey RJ, Molnar Z, *et al.* (2007). Mutations in alpha-tubulin cause abnormal neuronal migration in mice and lissencephaly in humans. Cell 128, 45–57.
Kelliher MT, Yue Y, Ng A, Kamiyama D, Huang B, Verhey KJ, Wildonger J (2018). Autoinhibition of kinesin-1 is essential to the dendrite-specific localization of Golgi outposts. J Cell Biol 217, 2531–2547.
Konishi Y, Stegmuller J, Matsuda T, Bonni S, Bonni A (2004). Cdh1-APC controls axonal growth and patterning in the mammalian brain. Science 303, 1026–1030.
Krijnse-Locker J, Parton RG, Fuller SD, Griffiths G, Dotti CG (1995). The organization of the endoplasmic reticulum and the intermediate compartment in cultured rat hippocampal neurons. Mol Biol Cell 6, 1315–1332.
Lim A, Rechtsteiner A, Saxton WM (2017). Two kinesins drive anterograde neuropeptide transport. Mol Biol Cell 28, 3542–3553.
Lipka J, Kapitein LC, Jaworski J, Hoogenraad CC (2016). Microtubule-binding protein doublecortin-like kinase 1 (DCLK1) guides kinesin-3-mediated cargo transport to dendrites. EMBO J 35, 302–318.
Liu JS, Schubert CR, Fu X, Fourniol FJ, Jaiswal JK, Houdusse A, Stultz CM, Moores CA, Walsh CA (2012). Molecular basis for specific regulation of neuronal kinesin-3 motors by doublecortin family proteins. Mol Cell 47, 707–721.
Miller PM, Folkmann AW, Maia AR, Efimova N, Efimov A, Kaverina I (2009). Golgi-derived CLASP-dependent microtubules control Golgi organization and polarized trafficking in motile cells. Nat Cell Biol 11, 1069–1080.
Mimori-Kiyosue Y, Grigoriev I, Lansbergen G, Sasaki H, Matsui C, Severin F, Galjart N, Grosveld F, Vorobjev I, Tsukita S, *et al.* (2005). CLASP1 and CLASP2 bind to EB1 and regulate microtubule plus-end dynamics at the cell cortex. J Cell Biol 168, 141–153.
Moores CA, Perderiset M, Francis F, Chelly J, Houdusse A, Milligan RA (2004). Mechanism of microtubule stabilization by doublecortin. Mol Cell 14, 833–839.
Moores CA, Perderiset M, Kappeler C, Kain S, Drummond D, Perkins SJ, Chelly J, Cross R, Houdusse A, Francis F (2006). Distinct roles of doublecortin modulating the microtubule cytoskeleton. EMBO J 25, 4448–4457.
Ori-McKenney KM, Jan LY, Jan YN (2012). Golgi outposts shape dendrite morphology by functioning as sites of acentrosomal microtubule nucleation in neurons. Neuron 76, 921–930.
Palmer KJ, Hughes H, Stephens DJ (2009). Specificity of cytoplasmic dynein subunits in discrete membrane-trafficking steps. Mol Biol Cell 20, 2885–2899.
Poirier K, Lebrun N, Broix L, Tian G, Saillour Y, Boscheron C, Parrini E, Valence S, Pierre BS, Oger M, *et al.* (2013). Mutations in TUBG1, DYNC1H1, KIF5C and KIF2A cause malformations of cortical development and microcephaly. Nat Genet 45, 639–647.
Rao S, Kirschen GW, Szczurkowska J, Di Antonio A, Wang J, Ge S, Shelly M (2018). Repositioning of Somatic Golgi Apparatus Is Essential for the Dendritic Establishment of Adult-Born Hippocampal Neurons. J Neurosci 38, 631–647.
Reiner O, Carrozzo R, Shen Y, Wehnert M, Faustinella F, Dobyns WB, Caskey CT, Ledbetter DH (1993). Isolation of a Miller-Dieker lissencephaly gene containing G protein beta-subunit-like repeats. Nature 364, 717–721.
Sarker KP, Wilson SM, Bonni S (2005). SnoN is a cell type-specific mediator of transforming growth factor-beta responses. J Biol Chem 280, 13037–13046.
Schaar BT, Kinoshita K, McConnell SK (2004). Doublecortin microtubule affinity is regulated by a balance of kinase and phosphatase activity at the leading edge of migrating neurons. Neuron 41, 203–213.
Shmueli A, Gdalyahu A, Sapoznik S, Sapir T, Tsukada M, Reiner O (2006). Site-specific dephosphorylation of doublecortin (DCX) by protein phosphatase 1 (PP1). Mol Cell Neurosci 32, 15–26.
Sun F, Zhu C, Dixit R, Cavalli V (2011). Sunday Driver/JIP3 binds kinesin heavy chain directly and enhances its motility. EMBO J 30, 3416–3429.
Tanaka T, Serneo FF, Higgins C, Gambello MJ, Wynshaw-Boris A, Gleeson JG (2004a). Lis1 and doublecortin function with dynein to mediate coupling of the nucleus to the centrosome in neuronal migration. J Cell Biol 165, 709–721.
Tanaka T, Serneo FF, Tseng HC, Kulkarni AB, Tsai LH, Gleeson JG (2004b). Cdk5 phosphorylation of doublecortin ser297 regulates its effect on neuronal migration. Neuron 41, 215–227.
Tsai JW, Lian WN, Kemal S, Kriegstein AR, Vallee RB (2010). Kinesin 3 and cytoplasmic dynein mediate interkinetic nuclear migration in neural stem cells. Nat Neurosci 13, 1463–1471.
Tsukada M, Prokscha A, Oldekamp J, Eichele G (2003). Identification of neurabin II as a novel doublecortin interacting protein. Mech Dev 120, 1033–1043.
Tsukada M, Prokscha A, Ungewickell E, Eichele G (2005). Doublecortin association with actin filaments is regulated by neurabin II. J Biol Chem 280, 11361–11368.
Vallee RB, McKenney RJ, Ori-McKenney KM (2012). Multiple modes of cytoplasmic dynein regulation. Nat Cell Biol 14, 224–230.
Vilela F, Velours C, Chenon M, Aumont-Nicaise M, Campanacci V, Thureau A, Pylypenko O, Andreani J, Llinas P, Menetrey J (2019). Structural characterization of the RH1-LZI tandem of JIP3/4 highlights RH1 domains as a cytoskeletal motor-binding motif. Sci Rep 9, 16036.
Wittmann T, Waterman-Storer CM (2005). Spatial regulation of CLASP affinity for microtubules by Rac1 and GSK3beta in migrating epithelial cells. J Cell Biol 169, 929–939.
Yadav S, Linstedt AD (2011). Golgi positioning. Cold Spring Harb Perspect Biol 3, a005322.
Yadav S, Puthenveedu MA, Linstedt AD (2012). Golgin160 recruits the dynein motor to position the Golgi apparatus. Dev Cell 23, 153–165.
Yang SZ, Wildonger J (2020). Golgi outposts locally regulate microtubule orientation in neurons but are not required for the overall polarity of the dendritic cytoskeleton. Genetics 215, 435–447.
Ye B, Zhang Y, Song W, Younger SH, Jan LY, Jan YN (2007). Growing dendrites and axons differ in their reliance on the secretory pathway. Cell 130, 717–729.
Zheng Y, Wildonger J, Ye B, Zhang Y, Kita A, Younger SH, Zimmerman S, Jan LY, Jan YN (2008). Dynein is required for polarized dendritic transport and uniform microtubule orientation in axons. Nat Cell Biol 10, 1172–1180.
Zhou W, Chang J, Wang X, Savelieff MG, Zhao Y, Ke S, Ye B (2014). GM130 is required for compartmental organization of dendritic golgi outposts. Curr Biol 24, 1227–1233.